Open access • Journal Article • DOI:10.1088/0029-5515/26/6/005

Features of spherical torus plasmas — Source link

Yueng Kay Martin Peng, Dennis J Strickler

Published on: 01 Jun 1986 - Nuclear Fusion (IOP Publishing)

Topics: Spherical tokamak, Reversed field pinch, Tokamak, Spheromak and Torus

LEGIBILITY NOTICE

A major purpose of the Technical Information Center is to provide the broadest dissemination possible of information contained in DOE's Research and Development Reports to business, industry, the academic community, and federal, state and local governments.

Although a small portion of this report is not reproducible, it is being made available to expedite the availability of information on the research discussed herein.

1

ORNL/FEDC-85/6

FEATURES OF SPHERICAL TORUS PLASMAS

Y-K. M. Peng
D. J. Strickler

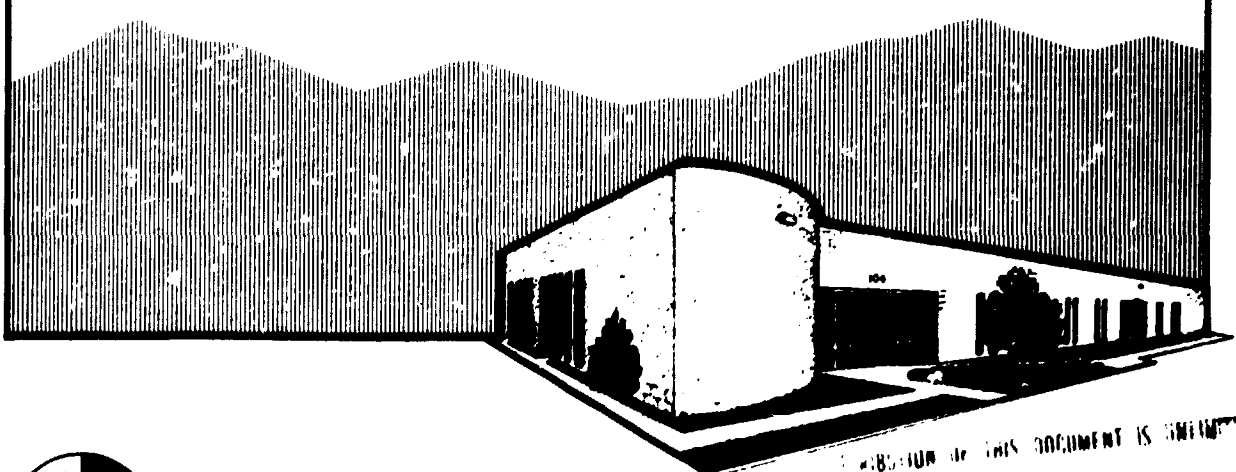

FUSION ENGINEERING DESIGN CENTER

OAK RIDGE NATIONAL LABORATORY   Operated by MARTIN MARIETTA ENERGY SYSTEMS, INC.

ORNL/FEDC-85/6
Dist. Category UC-20 c,d

ORNL/FEDC--85/6

DE86 004642

Fusion Energy Division

FEATURES OF SPHERICAL TORUS PLASMAS

Y-K. M. Peng and D. J. Strickler
Fusion Engineering Design Center

Date Published - December 1985

Prepared by the
OAK RIDGE NATIONAL LABORATORY
Oak Ridge, Tennessee 37831
operated by
MARTIN MARIETTA ENERGY SYSTEMS, INC.
for the
U.S. DEPARTMENT OF ENERGY
under Contract No. DE-AC05-84OR21400

CONTENTS

ABSTRACT

The spherical torus is a very small aspect ratio ($A < 2$) confinement concept obtained by retaining only the indispensable components inboard to the plasma torus. MHD equilibrium calculations show that spherical torus plasmas with safety factor $q > 2$ are characterized by high toroidal beta ($\beta_t > 0.2$), low poloidal beta ($\beta_p < 0.3$), naturally large elongation ($\kappa \geqslant 2$), large plasma current with $I_p/(aB_{t0})$ up to about 7 MA/mT, strong paramagnetism ($B_t/B_{t0} > 1.5$), and strong plasma helicity (F comparable to Θ). A large near-omnigeneous region is seen at the large-major-radius, bad-curvature region of the plasma in comparison with the conventional tokamaks. These features combine to engender the spherical torus plasma in a unique physics regime which permits compact fusion at low field and modest cost. Because of its strong paramagnetism and helicity, the spherical torus plasma shares some of the desirable features of spheromak and reversed-field pinch (RFP) plasmas, but with tokamak-like confinement and safety factor q. The general class of spherical tori, which includes the spherical tokamak ($q > 1$), the spherical pinch ($1 > q > 0$), and the spherical RFP ($q < 0$), have magnetic field configurations unique in comparison with conventional tokamaks and RFPs.

I. INTRODUCTION

High beta, good confinement, and steady-state operation in a compact configuration at modest field have long been major goals of magnetic fusion energy research. Accomplishing these in a single concept will permit cost-effective and attractive embodiments of future fusion reactors. The search for such a concept is of high interest in the present austere climate of fusion research. The introduction of the spherical torus concept[1] is to a large degree motivated by this search.

An equally important motivation of the spherical torus concept is its prospect of reducing the cost and time of fusion research and development. Examples of relatively cost-effective compact magnetic confinement experiments are already available. They include ZT-40M[2] and OHTE[3] for the RFP concept and S-1[4] and CTX[5] for the spheromak concept. In comparison with these alternative confinement concepts, a spherical torus experiment is expected to be similar in compactness, low field, and high beta, but better in its tokamak-like confinement time by more than an order of magnitude. This advantage should also be expected of the spherical torus devices for proof-of-principle, ignition, engineering development, or reactor prototype.

The idea of very small aspect ratio tokamaks, per se, has been advanced recently,[6,7] based primarily on conventional tokamak assumptions such as high poloidal beta, modest elongation, and inductive startup of the plasma current. In one case,[7] high beta was considered with β_p near unity, leading to beta values much higher than permitted by the more recent understanding of the first stability regime.[8,9] In contrast, the spherical torus projects high beta within the first stability regime through naturally large elongation and plasma current at a modest β_p. Its additional features of strong paramagnetism, near-omnigeneity,[10,11] strong helicity, and similarities to spheromaks and RFPs distinguish the spherical torus from these earlier concepts of small aspect ratio tokamaks.

The spherical torus concept is made plausible also by recent progress in advanced current drive schemes, such as initiation and rampup by lower hybrid waves[12,13] and maintenance by oscillating fields[14,15] (helicity injection[16,17]). This removes reliance on a full solenoid to induce the plasma current, permitting compact long-pulse spherical tori with aspect ratio significantly less than 2. Assuming these advanced current drive schemes, ignition spherical tori are estimated to be compact (R = 1.0 m to 1.6 m) and to operate at low fields (B_{t0} = 3 T to 2 T).[18] In the case of small, low-field, short-pulse experiments using pulsed high-current-density coils, full inductive current startup should remain feasible.

In the following, we discuss the unique features of spherical torus plasmas based primarily on their MHD equilibria, profiles, and magnetic configurations. This paper closes with a discussion of the questions and implications of our results for the spherical torus concept.

II. NATURAL ELONGATION

Free-boundary MHD equilibrium calculations show that an elongation of $\kappa = 2$ occurs naturally in a spherical torus with aspect ratio $A = 1.5$ when only a dipole vertical field is applied, which in this case is produced by two ring coils at a significant distance from the outboard side of the plasma [Figure 1(a)]. When a quadrupole shaping field is applied via coils above and below the plasma, an elongation of about 3 can be obtained [Figure 1(b)]. For $A > 2.5$ [Figures 1(c) and 1(d)], the natural plasma elongation is less than 1.4, and strong shaping coil currents are required to obtain elongations around 2.

A sequence of equilibria is obtained with an edge safety factor (inverse rotational transform) of $q_a = 2.4$ and A ranging from 3 to 1.5 while κ is increased from 1.7 (the usual elongation at large A) to 2. Poloidal field (PF) coils are placed at a distance of twice the minor radius ($2a$) from the plasma edge (Figure 2). The magnitudes of the coil

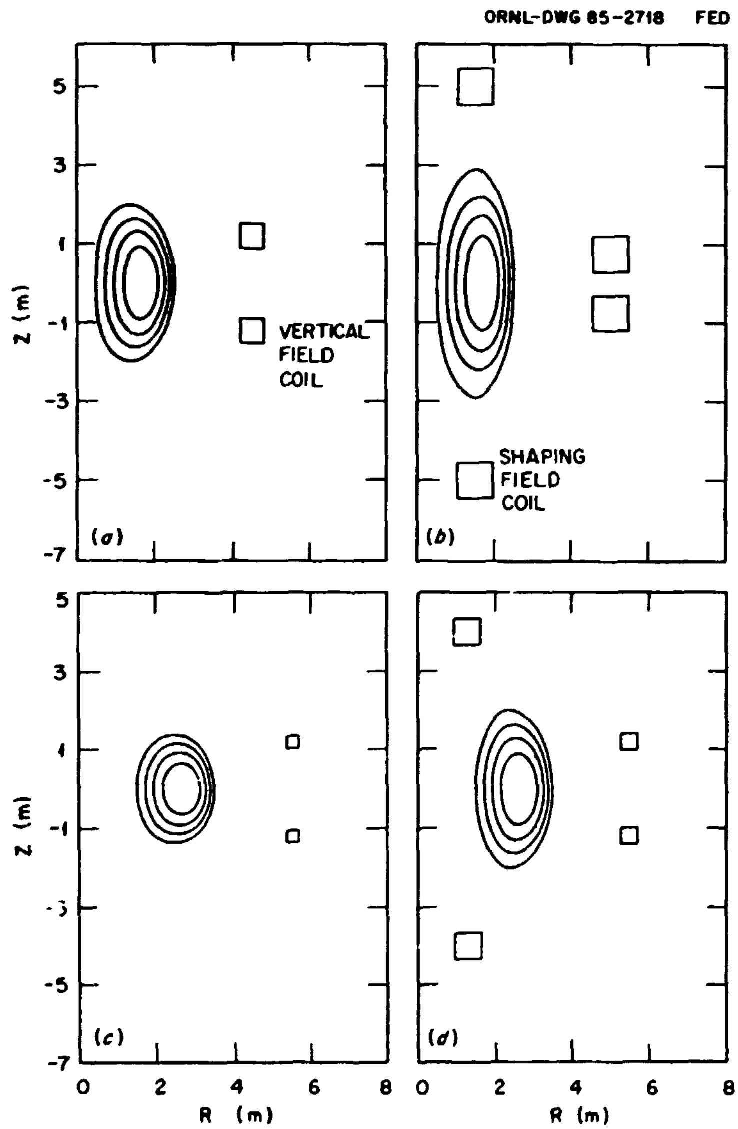

FIGURE 1. Naturally elongated and strongly elongated plasma cross sections at $A = 1.5$ (*a* and *b*, respectively), and at $A = 2.5$ (*c* and *d*, respectively).

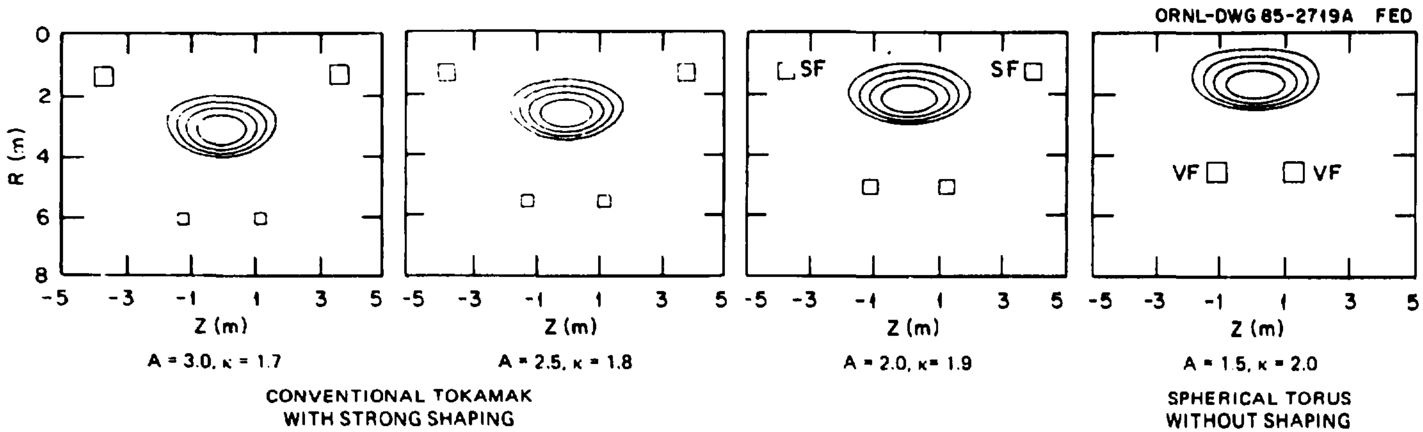

FIGURE 2. Variations of the generic poloidal field coils as the plasma changes from a naturally elongated spherical torus ($\kappa = 2$) at $A = 1.5$ to an elongated tokamak ($\kappa = 1.7$) at $A = 3$.

currents for these equilibria are plotted in Figure 3, showing that the vertical field (VF) current per coil relative to the plasma current, I_{VF}/I_p, decreases slightly from 0.4 to 0.3 as A decreases. However, the relative shaping field (SF) current, I_{SF}/I_p, decreases from 2.8 to 0 as A decreases from 4 to 1.5, resulting in a dramatic reduction in the total relative ampere-turns in the relatively faraway PF coils, $\sum |I_{PF}|/I_p$, from 6.4 to 0.6. The toroidal field (TF) coil ampere-turns, I_{TF}/I_p, also decreases drastically to levels comparable with the poloidal field ampere-turns. When a shaping field is applied to obtain a $\kappa = 3$ spherical torus, $\sum |I_{PF}|/I_p$ is seen to increase from 0.6 to about 1.2.

Large elongation (relative to that of tokamaks with conventional aspect ratios) is a natural feature of the spherical torus. These drastically reduced ampere-turns in a compact configuration should lead to substantial savings in the cost of the reactor magnet systems.

III. PLASMA CURRENT AND BETA

The typical profiles of the plasma pressure, toroidal current. and safety factor in these MHD equilibria are given in Figure 4, indicating a broad but not hollow current profile even with $q_0 = 1$ and $q_a = 2.4$. The equilibrium toroidal plasma current can be approximated by the formula:

$$I_p\,(\mathrm{MA}) = [5a\,(\mathrm{m})\,B_{t0}\,(\mathrm{T})/q_a]\,[C_I\,\epsilon/(1-\epsilon^2)^2]\,[(1+\kappa^2)/2]\ , \tag{1}$$

where B_{t0} is the vacuum toroidal field at the plasma major radius R, $\epsilon = 1/A$, and $C_I = 1.22 - 0.68\epsilon$. Thus, for a small spherical torus experiment with $R = 0.45$ m, $a = 0.27$ m, $\kappa = 2$, $q_a = 2.2$, and $B_{t0} = 0.5$ T, a plasma current of 0.9 MA is indicated. For this configuration with $q_a \geqslant 2.2$ we find that

$$I_p\,(\mathrm{MA})/[a\,(\mathrm{m})\,B_{t0}\,(\mathrm{T})] \leqslant 7\ , \tag{2}$$

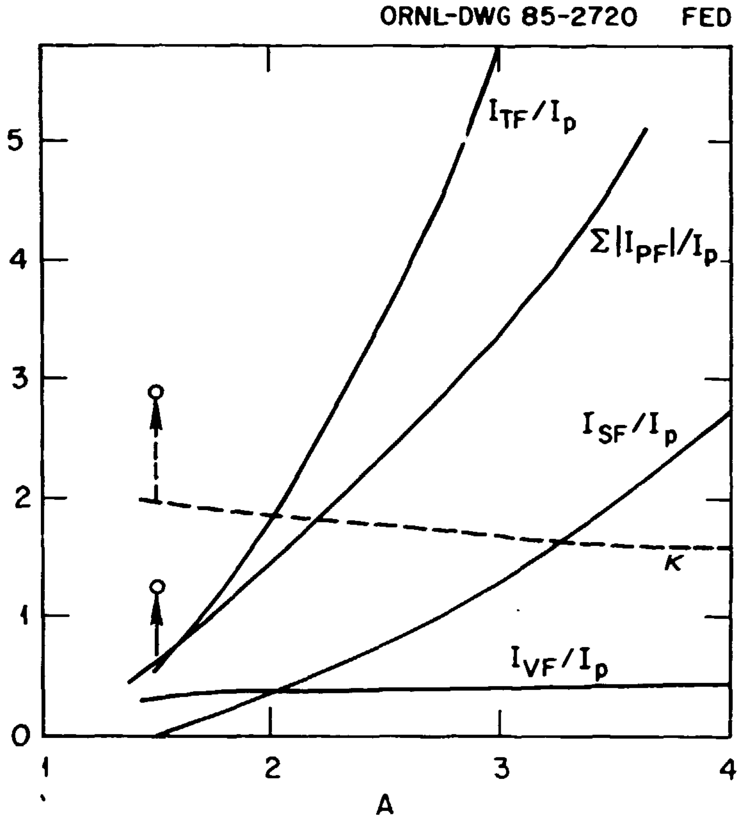

FIGURE 3. Dependence of vertical field (VF), shaping field (SF), poloidal field (PF), and toroidal field (TF) coil ampere-turns, relative to the plasma current, on the aspect ratio for the elongations indicated.

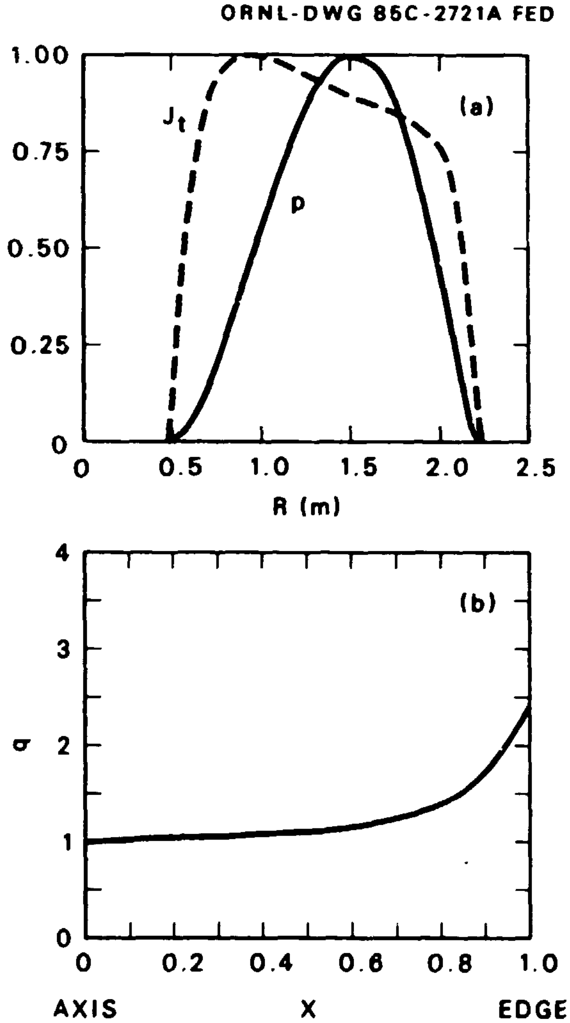

FIGURE 4. Typical profiles of plasma pressure $p(R)$, toroidal current density $J_t(R)$, and the safety factor $q(X)$, where X is the normalized poloidal flux, used in the equilibrium calculations.

which leads to a potential for high plasma beta in the first stability regime.[8,9] According to recent experimental indications,[19] the beta limit can be given approximately by:

$$\beta_c = \frac{2\mu_0\langle p\rangle}{B_{t0}^2} = 0.033\, I_p(\mathrm{MA})/[a\,(\mathrm{m})\, B_{t0}(\mathrm{T})] \;, \qquad (3)$$

indicating beta values above 20%. Unless otherwise mentioned, the equilibria presented in this paper have β_t values close to the β_c given here.

That such a high plasma current is permitted in a spherical torus can be seen in Figures 5 and 6. Figure 5 plots the poloidal and toroidal fields on the plasma mid-plane for a spherical torus ($A = 1.5$, $\kappa = 3$) and a conventional elongated tokamak plasma ($A = 2.5$, $\kappa = 1.8$). It is seen that in a spherical torus plasma the poloidal field becomes comparable with and larger than the toroidal field at the outboard region, while the fields are comparable in the inboard region. On the other hand, while the toroidal circumference at the outboard region is comparable with the poloidal circumference, the former is drastically shorter than the latter at the inboard region (Figure 6). As depicted by a field line plotted on the $q = 2$ surface, this gives highly pitched field lines at the outboard region, introducing only a small amount of toroidal rotation, but gives moderately pitched field lines at the inboard region, introducing a large amount of toroidal rotation. The net result is a strongly enhanced total toroidal rotation (higher q) for a given plasma current, or a higher plasma current for a given q_a. In comparison with this, a conventional tokamak permits only a small pitch to the field line for a given q, and hence a relatively modest plasma current. Equation (1) approximates this dependence on A.

That such a magnetic field configuration should give high beta for MHD stability can also be seen from Figure 6. In comparison with a conventional tokamak, the spherical torus has a short field line length in the bad-curvature region relative to that in the good-curvature region.

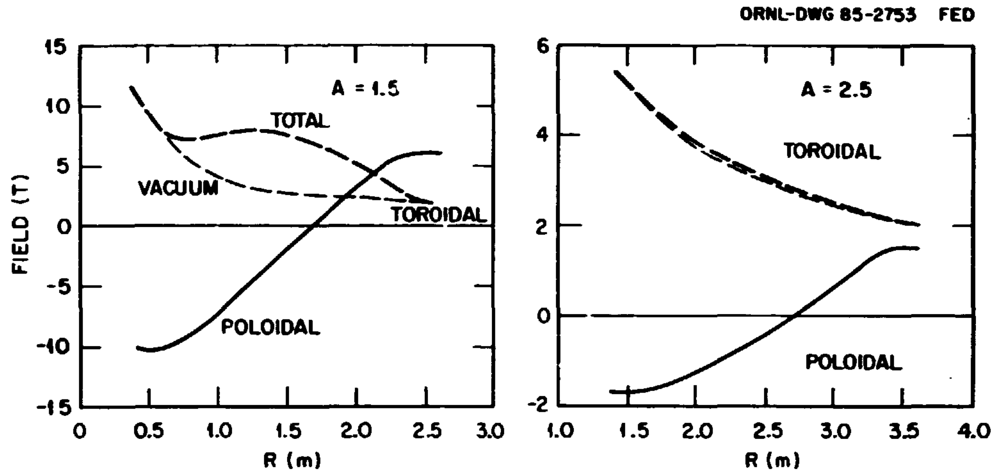

FIGURE 5. Distribution of the poloidal and toroidal fields on the plasma midplane of a spherical torus (A = 1.5, κ = 3) and a conventional tokamak (A = 2.5, κ = 1.8) with q_a = 2.4.

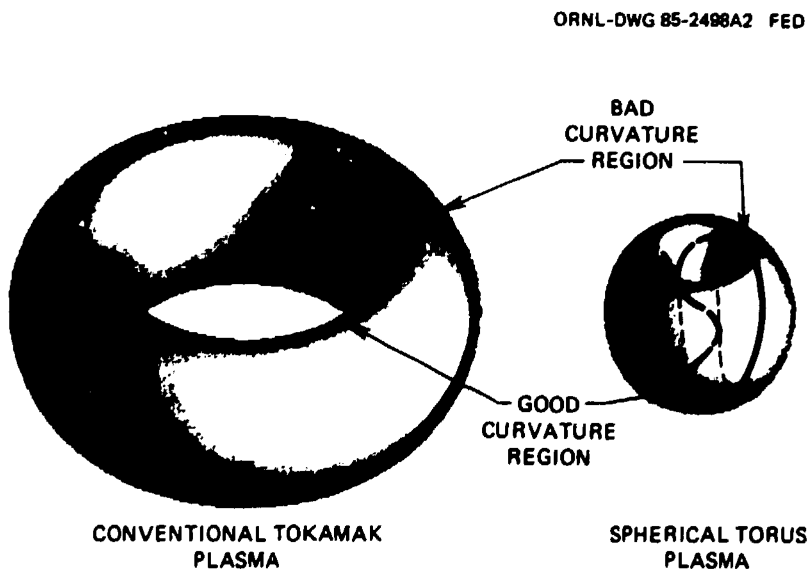

FIGURE 6. The contours of magnetic field lines on the q = 2 surfaces of a conventional tokamak and a spherical torus. The portion of the field lines in the good-curvature region is dashed.

IV. PLASMA PARAMAGNETISM

Defining the average poloidal field at the plasma edge, $\overline{B_p}$, as the line-averaged field along the poloidal circumference, the poloidal beta can be approximated by:

$$(\beta_p/\beta_t) = [5a\,(\mathrm{m})\,B_{t0}(\mathrm{T})/I_p\,(\mathrm{MA})]^2\,[(1 + \kappa^2)/2]\ . \qquad (4)$$

It can be seen that the poloidal beta should be around 0.3 and comparable to the limiting toroidal beta according to Equations (2) and (3). As a result, the plasma equilibrium is essentially force-free, that is, highly paramagnetic with the plasma current density, **J**, nearly parallel to the magnetic field. Since the magnetic field lines have a high pitch, a large poloidal current component is produced, leading to a strongly enhanced toroidal field, B_t, at the plasma axis. As indicated in Figure 5, (B_t/B_{t0}) is around 2 for a spherical torus, whereas it is within a few percent of unity in a conventional tokamak. Also, strong paramagnetism contributes to increasing the plasma current for a given q_0 via the increased toroidal field in the plasma core (see Sec. III).

The dependence of paramagnetism on the aspect ratio and the elongation is calculated and given in Figure 7. It is seen that, for a naturally elongated plasma, the plasma paramagnetism is significant only when A is less than 2, as long as $\beta \sim \beta_c$ according to Equation (3). For a strong elongation of about 3, significant paramagnetism sets in when A becomes less than 2.3. Since a highly pitched magnetic field line and a small poloidal beta are required for paramagnetism, a reduced I_p (an increased q) diminishes paramagnetism, and tends to regress a spherical torus to a conventional tokamak, even at a small aspect ratio (see also Figure 10). The presence of a strong paramagnetism thus serves as an indicator of the spherical torus characteristics.

Strong paramagnetism also introduces an important uncertainty in the application of Equation (3) in that the latter is based on data and calculations of plasmas where there is

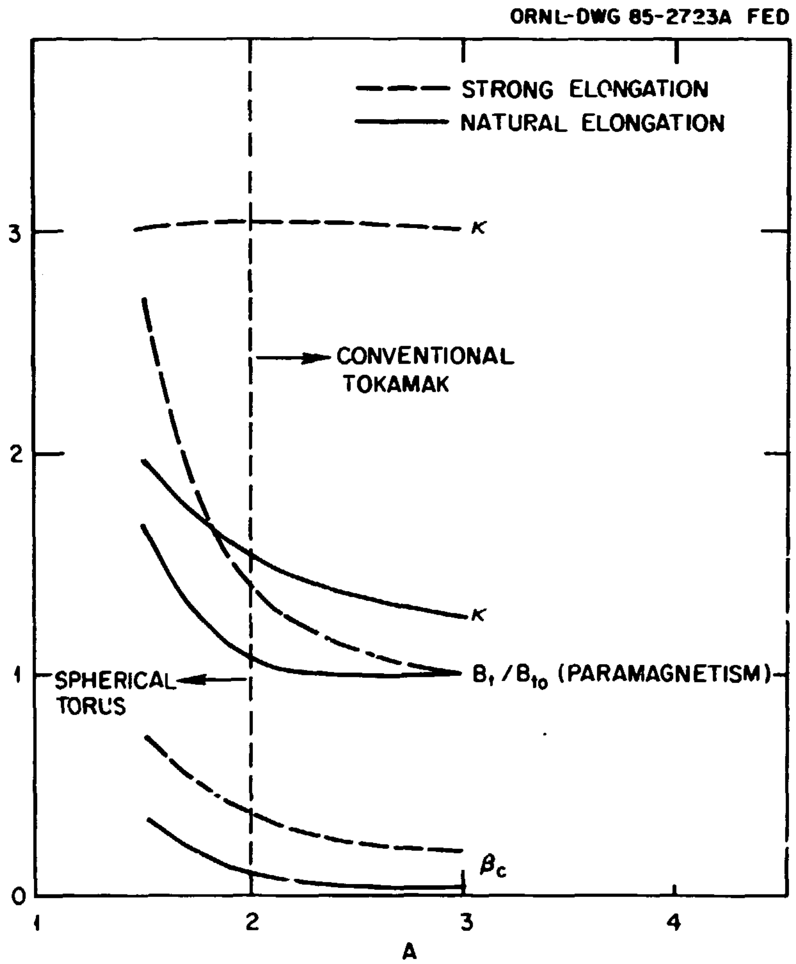

FIGURE 7. Dependence of paramagnetism (B_t/B_{t0}) and critical beta (β_c) on aspect ratio for strongly elongated plasmas (κ = 3) and naturally elongated plasmas.

negligible difference between B_{t0} and B_t at the plasma axis. Replacing both B_{t0}'s in Equation (3) by B_t would lead to an increase of the plasma pressure at the limiting beta by a factor of (B_t/B_{t0}). When only one of the B_{t0}'s is replaced by B_t, the range of uncertainty in pressure becomes proportional to $(B_t/B_{t0})^3$. However, since paramagnetism decreases with increasing plasma pressure, the range of this uncertainty is limited to $\beta_p < 1$.

V. NEAR-OMNIGENEITY[10,11]

The strong paramagnetism of the spherical torus introduces a magnetic configuration that is dramatically different from that of a conventional tokamak. As shown in Figure 8, the strongly enhanced B_t at the plasma core and the dominating poloidal field at the outboard region of the plasma create a strong curvature of the surfaces of constant field strength, $|B|$, making them largely parallel to the flux surfaces there. In this region, the particle drift orbits coincide with the flux surfaces since the curvature and gradient drifts[20] are now parallel to the flux surfaces.

This nearly omnigeneous region (Figure 8) largely coincides with the region of bad curvature of MHD instability where the pressure gradient and the field line curvature, $\mathbf{B} \cdot \nabla \mathbf{B}$, have positive scalar product. This region is nearly free of locally trapped particles, contributing to the kinetic stability of the plasma, although trapped particles still exist between the top and bottom regions of the plasma. These trapped particles have orbits that deviate weakly from the flux surfaces because of the reduced region where the curvature and gradient drifts deviate from the parallel drift. This should result in a reduced "banana" width and is expected to lead to a reduced neoclassical transport.

It should be noted that this region of near-omnigeneity is also characterized by a near-constancy of $|B|$. This can be seen in Figure 9, where the VF coils are placed somewhat closer to the plasma, introducing some finer structures to the surfaces of constant $|B|$. Although this may introduce additional features to the trapped-particle orbits, the

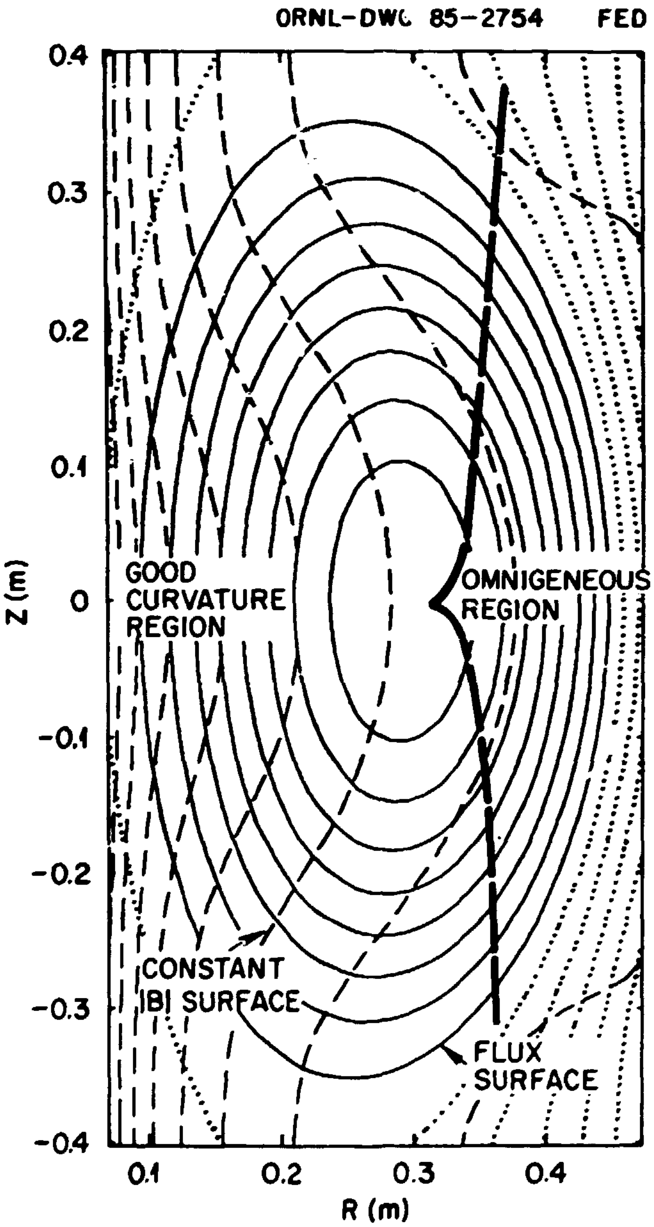

FIGURE 8. Configurations of spherical torus plasma flux surfaces (solid and dotted lines) and $|B|$-surfaces (dashed lines). The near-omnigeneous region is to the right of the bold dashed line.

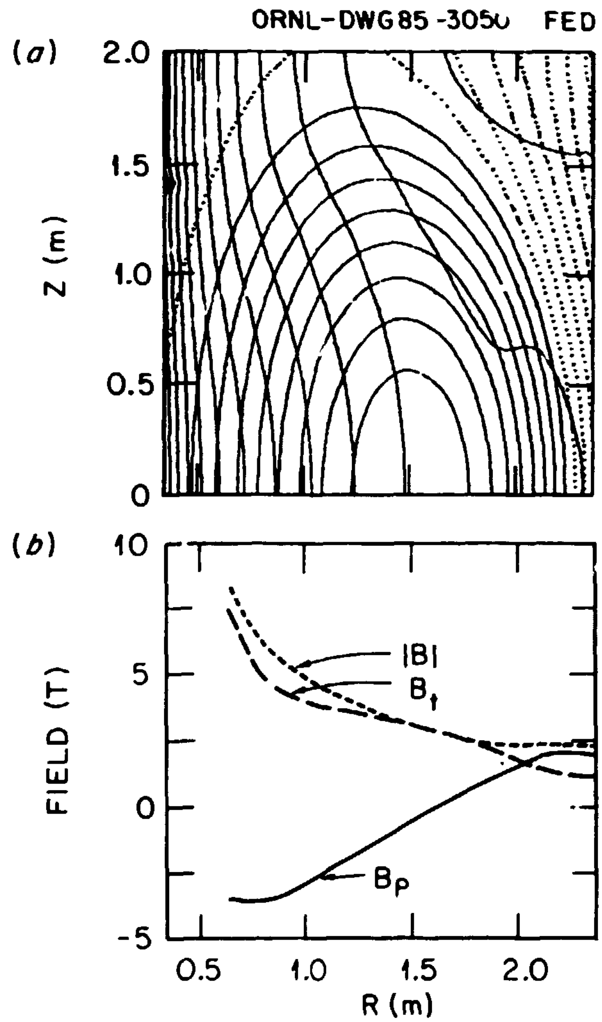

FIGURE 9. (*a*) $|B|$-surfaces and flux surfaces of a spherical torus with $q_a = 2.4$ and nearby vertical field coils, and (*b*) the distribution of B_p, B_t, and $|B|$ on the plasma midplane over the major radius.

near-constancy of $|B|$ should retain the near-omnigeneity of this region. Since the size of the region depends on plasma elongation, beta, and paramagnetism, it is subject to external controls of the shaping field, plasma heating, and safety factor (plasma current).

VI. PLASMA HELICITY

Toroidal plasma helicity can be expressed by the helicity parameter Θ:[21]

$$\Theta = \langle B_p \rangle_S / \langle B_t \rangle_V \ , \qquad (5)$$

where the subscripts S and V indicate surface and volume averages, respectively, of a toroidal plasma. As the plasma current increases in a spherical torus configuration (A = 1.6, κ = 2), the plasma evolves from a low-current (high-q), weakly paramagnetic configuration to a high-current (low-q), strongly paramagnetic configuration. This transformation can be depicted in the F-Θ space (Figure 10), where F (the pinch parameter) represents the relative toroidal field strength at the plasma surface:

$$F = \langle B_t \rangle_S / \langle B_t \rangle_V \ . \qquad (6)$$

As Θ increases, F decreases from near 1 because of the increasing paramagnetism, a trend consistent with the indications of the Bessel function approximation[21] of the force-free cylindrical configuration. Preliminary calculations of the values of F and Θ in a spherical torus with $q_a > 1$ suggest that they are comparable in magnitude, indicating a strong plasma helicity. This strong helicity is consistent with the nature of the field line contours depicted in Figure 6.

Although current drive via ac helicity injection (oscillating field) was first introduced for the RFP[14] and spheromak,[15] its application to tokamak plasmas was also suggested

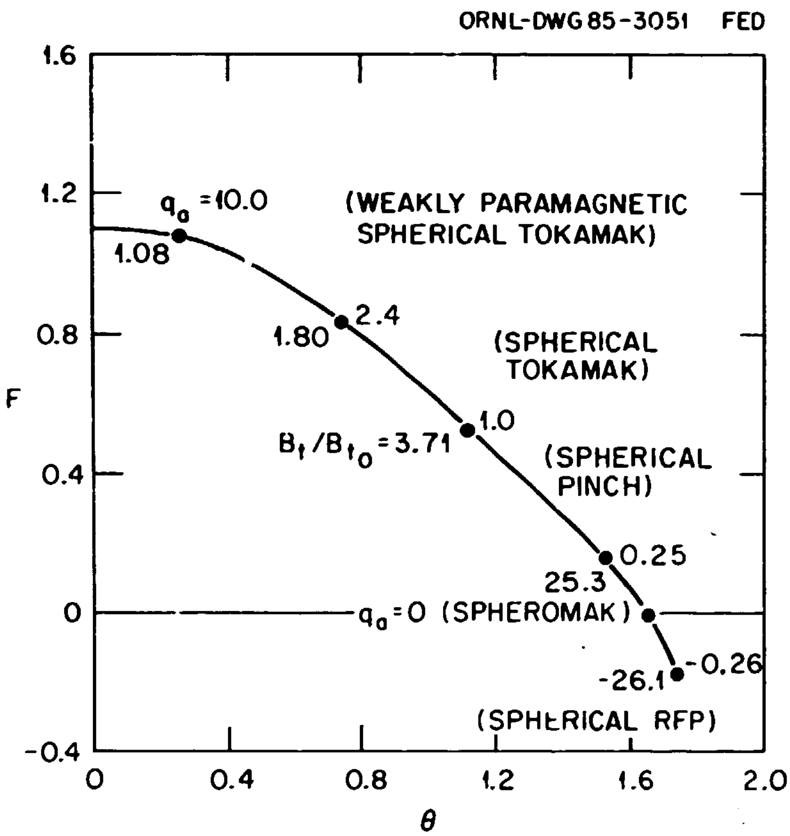

FIGURE 10. The plasma pinch parameter, $F = \langle B_t \rangle_S / \langle B_t \rangle_V$, as a function of plasma helicity, $\Theta = \langle B_p \rangle_S / \langle B_t \rangle_V$, for spherical tori with $A = 1.5$, $I_p = 10$ MA, and $R = 1.5$ m, spanning spherical tokamak with $q_a > 1$, spherical pinch with $0 < q_a < 1$, spheromak with $q_a = 0$, and spherical RFP with $q_a < 0$.

recently.[16,17] The efficacy of this process in spherical tori is enhanced by the following factors. First, the total stored magnetic flux is modest relative to the plasma energy content (high beta and low field). Second, in the cylindrical approximation of an RFP, the induced toroidal loop voltage increases with increasing $(1 - F)$ and increasing Θ,[22] suggesting that the efficiency of ac helicity injection in a spherical torus should be of the same order of magnitude as in an RFP.

VII. CLASSES OF SPHERICAL TORI

As the value of B_{t0} is reduced relative to the plasma current (with q_a reduced to <1), plasma paramagnetism is further enhanced because of the increased pitch of the magnetic field line. This gedanken process can in principle be continued through $B_{t0} = 0$ and beyond to $B_{t0} < 0$. An example of a spherical torus with $q_a < 0$ is shown in Figure 11, indicating that the plasma retains its naturally large elongation, and that the $|B|$-surfaces are drastically different in configuration from those of a spherical torus of $q_a > 1$. Near-omnigeneity in the outboard region of the plasma appears to be a feature unique to the spherical torus with $q > 1$.

The following classes of spherical tori are therefore evident:

1. spherical tokamak with $q_a > 1$,
2. spherical pinch with $1 > q_a > 0$,
3. spheromak with $q_a = 0$, and
4. spherical RFP with $q_a < 0$.

The domains of these different classes of spherical tori relative to the tokamak, spheromak, and RFP are depicted in Figure 12.

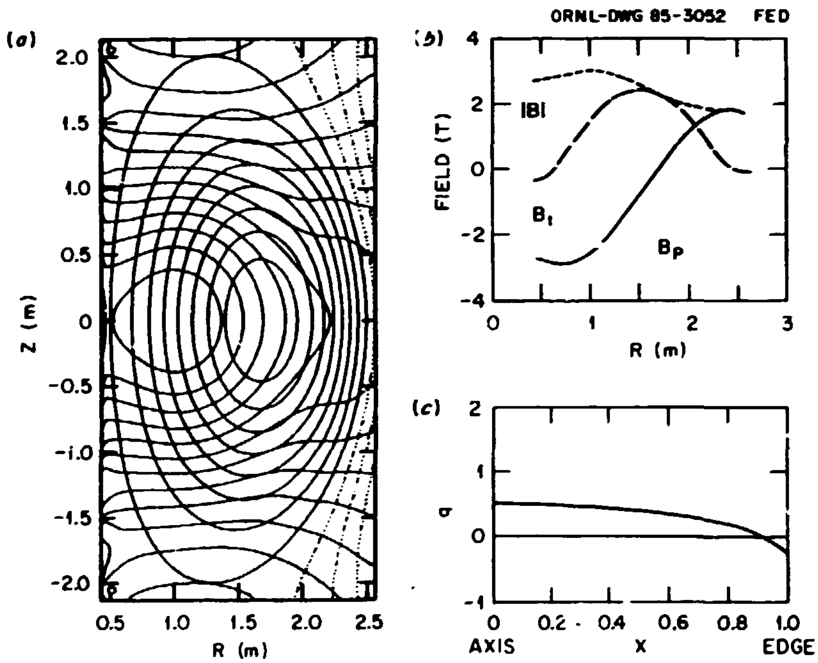

FIGURE 11. (*a*) Flux and $|B|$-surfaces for a spherical RFP with $q_a = -0.26$, with (*b*) its magnetic field distributions on the plasma midplane, and (*c*) its q profile as a function of normalized poloidal flux, X.

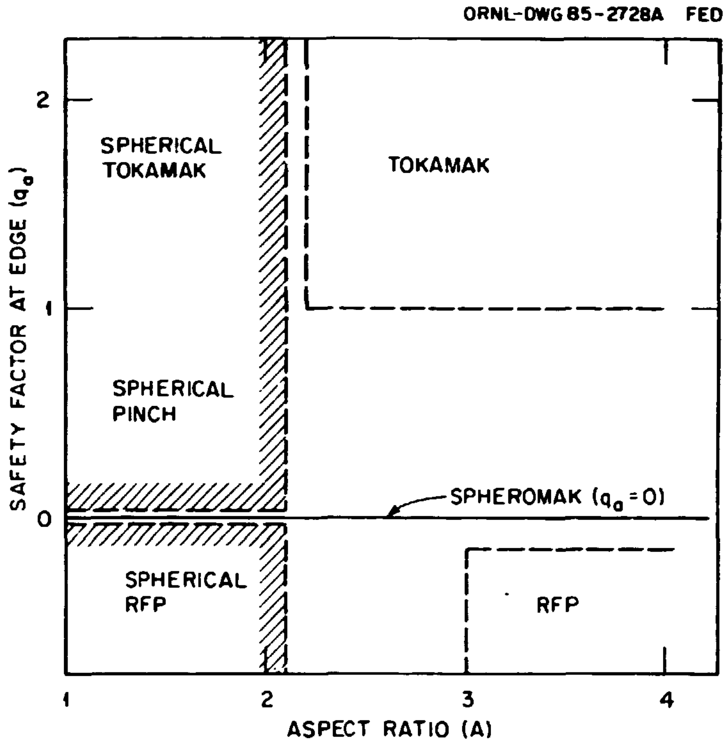

FIGURE 12. The domain of spherical tori (spherical tokamak, spherical pinch, and spherical RFP) relative to those of tokamak, spheromak, and RFP in the q_a and A space.

VIII. DISCUSSION

Although the features of the spherical torus plasmas discussed here are based only on a limited number of MHD equilibria, they appear qualitatively different from the conventional tokamak plasmas in the case of $q_a > 1$. These features include naturally large elongation, large plasma current, high beta in the first stability regime, low poloidal beta, comparable toroidal and poloidal fields, strong paramagnetism, near-omnigeneity, and strong helicity. Because results are exceptionally interesting so far, independent calculations with a broader range of the assumed input profile functions and parameters are encouraged.

In discussing the implications of these plasma features, much of the conventional wisdom of the toroidal plasma physics is applied here. Since there is no concrete data base for spherical tori, our discussions serve primarily to indicate possible important directions of theoretical analysis and experimental testing. Examples include the uncertainties in the effects of strong paramagnetism on achievable plasma beta; the effects of near-omnigeneity on plasma kinetic properties; plasma energy confinement at tight aspect ratio and high current; the efficacy of lower hybrid wave and oscillating field current drive approaches; and the viability of the spherical pinch and spherical RFP configurations. The attractiveness of the spherical torus as a compact magnetic fusion concept depends on the resolution of questions such as these.

Acknowledgments

One of the authors (Y-K. M. Peng) wishes to thank T. E. Shannon for his initial interest in and stimulating discussions on the engineering concepts of the spherical torus. He further wishes to thank J. Sheffield and E. A. Lazarus for discussions on the physics issues of the Spherical Torus Experiment (STX), which embodies many of the results discussed in this paper. The authors thank J. B. Miller for computational support.

References

1. Y-K. M. Peng, *Spherical Torus, Compact Fusion at Low Field*, Oak Ridge National Laboratory Report ORNL/FEDC-84/7, Oak Ridge, Tennessee (January 1985).

2. D. A. Baker *et al.*, "Experimental and Theoretical Studies of the ZT-40M Reversed-Field Pinch," in *Proc. 12th Int. Conf. on Plasma Phys. Contr. Nucl. Fusion Res., 1984* (IAEA, Vienna, 1985) Vol. II, p. 439.

3. T. Tamano *et al.*, "High-Current High-Beta Toroidal Pinch Experiments on OHTE," in *Proc. 12th Int. Conf. on Plasma Phys. Contr. Nucl. Fusion Res., 1984* (IAEA, Vienna, 1985) Vol. II, p. 431.

4. M. Yamada *et al.*, "Initial Results from S-1 Spheromak," in *Proc. 12th Int. Conf. on Plasma Phys. Contr. Nucl. Fusion Res., 1984* (IAEA, Vienna, 1985) Vol. II, p. 535.

5. T. R. Jarboe *et al.*, "Spheromak Studies on CTX," in *Proc. 12th Int. Conf. on Plasma Phys. Contr. Nucl. Fusion Res., 1984* (IAEA, Vienna, 1985) Vol. II, p. 501.

6. D. L. Jassby, Comm. Plasma Phys. and Contr. Fusion 3, 151 (1978).

7. Y-K. M. Peng and R. A. Dory, *Very Small Aspect Ratio Tokamak*, Oak Ridge National Laboratory Report ORNL/TM-6535, Oak Ridge, Tennessee (October 1978).

8. A. Sykes *et al.*, in *Proc. 11th Europ. Conf. on Plasma Phys. and Contr. Fusion Res., Aachen, 1983* (European Phys. Soc., 1984), Vol. VIID, Part II, p. 363.

9. F. Troyon *et al.*, in *Proc. 11th Europ. Conf. on Plasma Phys. Contr. Nucl. Fusion Res., Aachen, 1983* (European Phys. Soc., 1984), Vol. XXVI, No. 1A, p. 209.

10. D. Palumbo, Nuovo Cimento **53, Part B**, 507 (1968).

11. P. J. Catto and R. D. Hazeltine, Phys. Rev. Lett. **46**, 1002 (1981).

12. N. J. Fisch and C. F. F. Karney, *Current Ramp-up With RF Waves in a Tokamak*, Princeton Plasma Physics Laboratory Report PPPL-2132, Princeton, New Jersey (1984).

13. C. F. F. Karney, *Comparison of the Theory and the Practice of RF Current Drive,* Princeton Plasma Physics Laboratory Report PPPL-2152, Princeton, New Jersey (1984).

14. K. F. Schoenberg *et al.*, J. Appl. Phys. **56**, 2519 (1984).

15. A. Janos, *Steady State Operation Spheromak by Inductive Techniques,* Princeton Plasma Physics Laboratory Report PPPL-2095, Princeton, New Jersey (August 1984).

16. T. H. Jensen and M. S. Chu, *Current Drive and Helicity Injection,* GA Technologies Report GA-A17424, San Diego, California (November 1983).

17. P. M. Bellan, Phys. Fluids **27**, 2191 (1984).

18. Y-K. M. Peng *et al.*, "Spherical Torus: An Approach to Compact Fusion at Low Field—Initial Ignition Assessments," paper presented at the Sixth Topical Meeting on Technology of Fusion Energy, March 3–7, 1985, San Francisco (to the published in Fusion Technol.).

19. R. D. Stambaugh *et al.*, "Test of Beta Limits as a Function of Plasma Shape in the Doublet III Device," in *Proc. 12th Int. Conf. on Plasma Phys. and Contr. Nucl. Fusion Res., 1984* (IAEA, Vienna 1985), Vol. I, p. 217.

20. D. J. Rose and M. Clark, Jr., in *Plasmas and Controlled Fusion* (The M.I.T. Press, Cambridge, Massachusetts, 1961), Chap. 10.

21. J. B. Taylor, Phys. Rev. Lett. **33**, 1139 (1974).

22. R. L. Hagenson *et al.*, *Compact Reversed-Field Pinch Reactor (CRFPR): Preliminary Engineering Considerations,* Los Alamos National Laboratory Report LA-10200-MS, Los Alamos, New Mexico (August, 1984).

ORNL/FEDC-85/6
Dist. Category UC-20 c,d

INTERNAL DISTRIBUTION

1. R. J. Barrett
2. D. B. Batchelor
3. D. D. Bates
4. C. O. Beasley
5. W. R. Becraft
6. D. T. Blackfield
7. T. G. Brown
8. R. D. Burris
9. C. E. Bush
10. B. A. Carreras
11. R. E. Clausing
12. R. J. Colchin
13. W. A. Cooper
14. E. C. Crume
15. R. A. Dory
16. J. L. Dunlap
17. G. R. Dyer
18. P. H. Edmonds
19. A. C. England
20. W. A. Gabbard
21. J. D. Galambos
22. L. Garcia
23. J. C. Glowienka
24. G. E. Gorker
25. J. H. Harris
26. H. H. Haselton
27. D. E. Hastings
28. C. L. Hedrick
29. D. L. Hillis
30. S. P. Hirshman
31. J. T. Hogan
32. W. A. Houlberg
33. H. C. Howe
34. R. C. Isler
35. E. F. Jaeger
36. T. C. Jernigan
37. S. S. Kalsi
38. P. W. King
39. R. A. Langley
40. E. A. Lazarus
41. V. D. Lee
42. D. C. Lousteau
43. M. S. Lubell
44. J. F. Lyon
45. C. H. Ma
46. J. B. Miller
47. S. L. Milora
48. P. K. Mioduszewski
49. M. Murakami
50. G. H. Neilson
51. W. D. Nelson
52. V. K. Pare
53–57. Y-K. M. Peng
58. D. A. Rasmussen
59. R. L. Reid
60. R. K. Richards
61. B. W. Riemer
62. E. Rodriguez-Solano
63. J. A. Rome
64. M. J. Saltmarsh
65. E. C. Selcow
66. K. C. Shaing
67. T. E. Shannon
68. J. Sheffield
69. D. J. Sigmar
70. P. T. Spampinato
71. D. A. Spong
72. W. L. Stirling
73–77. D. J. Strickler
78. D. W. Swain
79. G. E. Taylor
80. C. C. Tsai
81. N. A. Uckan
82. J. W. Whealton
83. J. B. Wilgen
84. W. R. Wing
85. J. J. Yugo
86. R. A. Zuhr
87–88. Laboratory Records Department
89. Laboratory Records, ORNL-RC
90. Central Research Library
91. Document Reference Section
92. Fusion Energy Division Library
93. Fusion Energy Division Publications Office
94. ORNL Patent Office

EXTERNAL DISTRIBUTION

95. M. A. Abdou, Boelter Hall, University of California, Los Angeles, CA 90024
96. C. A. Anderson, Westinghouse Electric Corporation, Advanced Energy Energy Systems Division, P.O. Box 158, Madison, PA 15663
97. J. L. Anderson, CMB-3, Mail Stop 348, Los Alamos National Laboratory, P.O. Box 1633, Los Alamos, NM 87545
98. C. C. Baker, FPP/208, Argonne National Laboratory, 9700 South Cass Avenue, Argonne, IL 60439
99. D. S. Beard, Office of Fusion Energy, Office of Energy Research, ER-531 Germantown, U.S. Department of Energy, Washington, DC 20545
100. K. L. Black, Department E452, McDonnell Douglas Astronautics Company, P.O. Box 516, St. Louis, MO 63166
101. R. Botwin, C47-05, Grumman Aerospace Corporation, P.O. Box 31, Bethpage, NY 11714
102. W. B. Briggs, McDonnell Douglas Astronautics Company, P.O. Box 516, St. Louis, MO 63166
103. J. N. Brooks, FPP/207, Argonne National Laboratory, 9700 South Cass Avenue, Argonne, IL 60439
104. S. C. Burnett, GA Technologies, Inc., P.O. Box 81608, San Diego, CA 92138
105. J. D. Callen, Department of Nuclear Engineering, University of Wisconsin, Madison, WI 53706
106. R. N. Cherdack, Burns and Roe, Inc., 800 Kinderkamack Road, Oradell, NJ 07649
107. D. R. Cohn, MIT Plasma Fusion Center, 167 Albany Street, Cambridge, MA 02139
108. J. W. Coursen, C36-05, Grumman Aerospace Corporation, P.O. Box 31, Bethpage, NY 11714
109. R. W. Conn, School of Chemical, Nuclear, and Thermal Engineering, Boelter Hall, University of California, Los Angeles, CA 90024
110. J. G. Crocker, EG&G Idaho, P.O. Box 1625, Idaho Falls, ID 83401
111. G. R. Dalton, Department of Nuclear Engineering Science, Nuclear Science Center, University of Florida, Gainesville, FL 32611
112. R. C. Davidson, Massachusetts Institute of Technology, 77 Massachusetts Avenue, Cambridge, MA 02139
113. N. A. Davies, Office of Fusion Energy, Office of Energy Research, ER-51 Germantown, U.S. Department of Energy, Washington, DC 20545
114. S. O. Dean, Director, Fusion Energy Development, Science Applications International Corporation, 2 Professional Drive, Suite 249, Gaithersburg, MD 20760
115. D. DeFreece, E451, Building 81/1/B7, McDonnell Douglas Astronautics Company, P.O. Box 516, St. Louis, MO 63166
116. J. N. Doggett, L-441, Lawrence Livermore National Laboratory, P.O. Box 5511, Livermore, CA 94550
117. H. Dreicer, Division Leader, CRT, Los Alamos National Laboratory, P.O. Box 1663, Los Alamos, NM 87545
118. D. Ehst, Argonne National Laboratory, 9700 South Cass Avenue, Argonne, IL 60439
119. F. Farfaletti-Casali, Engineering Division, Joint Research Center, Ispra Establishment, 21020 Ispra (Varese), Italy
120. P. A. Finn, Fusion Power Program, Argonne National Laboratory, 9700 South Cass Avenue, Argonne, IL 60439
121. H. K. Forsen, Bechtel Group, Inc., Research & Engineering, P.O. Box 3965, San Francisco, CA 94119
122. J. S. Foster, Jr., Building R4-2004, TRW Defense and Space Systems, 1 Space Park, Redondo Beach, CA 90278

123. T. K. Fowler, Associate Director for Magnetic Fusion Energy, L-436, Lawrence Livermore National Laboratory, P.O. Box 5511, Livermore, CA 94550
124. J. W. French, Princeton Plasma Physics Laboratory, P.O. Box 451, Princeton, NJ 08544
125. H. P. Furth, Director, Princeton Plasma Physics Laboratory, P.O. Box 451, Princeton, NJ 08544
126. J. G. Gavin, Jr., President, A01-11, Grumman Aerospace Corporation, P.O. Box 31, Bethpage, NY 11714
127. S. K. Ghose, Lawrence Livermore National Laboratory, P.O. Box 5511, Livermore, CA 94550
128. G. Gibson, Westinghouse Electric Corporation, Fusion Power Systems Department, P.O. Box 10864, Pittsburgh, PA 15236
129. J. R. Gilleland, Manager, Fusion Project, GA Technologies, Inc., P.O. Box 81608, San Diego, CA 92138
130. M. Y. Gohar, Argonne National Laboratory, 9700 South Cass Avenue, Argonne, IL 60439
131. R. W. Gould, Department of Applied Physics, California Institute of Technology, Pasadena, CA 91109
132. M. W. Griffin, Department E236, McDonnell Douglas Astronautics Company, P.O. Box 516, St. Louis, MO 63166
133. R. A. Gross, Plasma Research Laboratory, Columbia University, New York, NY 10027
134. J. R. Haines, McDonnell Douglas Astronautics Company, St. Louis, MO 63166
135. C. D. Henning, Lawrence Livermore National Laboratory, P.O. Box 5511, Livermore, CA 94550
136. J. J. Holmes, Westinghouse-Hanford Engineering Development Laboratory, P.O. Box 1970, Richland, WA 99352
137. D. Hwang, Princeton Plasma Physics Laboratory, P.O. Box 451, Princeton, NJ 08544
138. J. B. Joyce, Princeton Plasma Physics Laboratory, P.O. Box 451, Princeton, NJ 08544
139. R. A. Krakowski, CTR-12, Mail Stop 641, Los Alamos National Laboratory, P.O. Box 1663, Los Alamos, NM 87545
140. G. L. Kulcinski, University of Wisconsin, Department of Nuclear Engineering, Engineering Research Building, Room 439, 1500 Johnson Drive, Madison, WI 53706
141. D. L. Kummer, McDonnell Douglas Astronautics Company, P.O. Box 516, St. Louis, MO 63166
142. W. Marton, Office of Fusion Energy, Office of Energy Research, ER-55 Germantown, U.S. Department of Energy, Washington, DC 20545
143. L. G. Masson, EG&G Idaho, Idaho National Engineering Laboratory, P.O. Box 1625, Idaho Falls, ID 83401
144. D. M. Meade, Princeton Plasma Physics Laboratory, P.O. Box 451, Princeton, NJ 08544
145. A. T. Mense, Building 107, Post B2, McDonnell Douglas Astronautics Company, P.O. Box 516, St. Louis, MO 63166
146. R. W. Moir, Lawrence Livermore Laboratory, P.O. Box 5511, Livermore, CA 94550
147. D. B. Montgomery, MIT Plasma Fusion Center, 167 Albany Street, Cambridge, MA 02139
148. A. E. Munier, Grumman Aerospace Corporation, P.O. Box 31, Bethpage, NY 11714
149. R. E. Nygren, FPP/207, Argonne National Laboratory, 9700 South Cass Avenue, Argonne, IL 60439
150. T. Ohkawa, GA Technologies, Inc., P.O. Box 81608, San Diego, CA 92138
151. J. A. O'Toole, Plasma Physics Laboratory, James Forrestal Campus, Building I-P, Room 8A, P.O. Box 451, Princeton, NJ 08544
152. R. R. Parker, Francis Bitter National Magnet Laboratory, 170 Albany Street, Cambridge, MA 02139
153. B. Pease, Culham Laboratory, Abingdon, Oxfordshire OX14 3DB, United Kingdom
154. M. Pelovitz, Princeton Plasma Physics Laboratory, P.O. Box 451, Princeton, NJ 08544

155. F. W. Perkins, Princeton Plasma Physics Laboratory, P.O. Box 451, Princeton, NJ 08544
156. M. Porkolab, Massachusetts Institute of Technology, 77 Massachusetts Avenue, Cambridge, MA 02139
157. D. E. Post, Princeton Plasma Physics Laboratory, P.O. Box 451, Princeton, NJ 08544
158. R. E. Price, Office of Fusion Energy, Office of Energy Research, ER-55 Germantown, U.S. Department of Energy, Washington, DC 20545
159. F. A. Puhn, GA Technologies, Inc., P.O. Box 81608, San Diego, CA 92138
160. J. Purcell, GA Technologies, Inc., P.O. Box 81608, San Diego, CA 92138
161. R. V. Pyle, University of California, Lawrence Berkeley Laboratory, Berkeley, CA 94720
162. J. M. Rawls, GA Technologies, Inc., P.O. Box 81608, San Diego, CA 92138
163. M. Roberts, Office of Fusion Energy, ER-52 Germantown, U.S. Department of Energy, Washington, DC 20545
164. J. D. Rogers, Los Alamos National Laboratory, P.O. Box 1663, Los Alamos, NM 87545
165. M. L. Rogers, Monsanto Research Corporation, Mound Laboratory Facility, P.O. Box 32, Miamisburg, OH 45342
166. M. N. Rosenbluth, RLM 11.218, Institute for Fusion Studies, University of Texas, Austin, TX 78712
167. P. H. Rutherford, Princeton Plasma Physics Laboratory, P.O. Box 451, Princeton, NJ 08544
168. J. A. Schmidt, Princeton Plasma Physics Laboratory, P.O. Box 451, Princeton, NJ 08544
169. J. Schultz, MIT Plasma Fusion Center, 167 Albany Street, Cambridge, MA 02139
170. F. R. Scott, Electric Power Research Institute, P.O. Box 10412, Palo Alto, CA 94304
171. G. Sheffield, Princeton Plasma Physics Laboratory, P.O. Box 451, Princeton, NJ 08544
172. D. Smith, Materials Science Division, Argonne National Laboratory, 9700 South Cass Avenue, Argonne, IL 60439
173. W. M. Stacey, Jr., Georgia Institute of Technology, School of Nuclear Engineering and Health Physics, Atlanta, GA 30332
174. D. Steiner, Rensselaer Polytechnic Institute, Nuclear Engineering Department, NES Building, Tibbets Avenue, Troy, NY 12181
175. E. Stern, Grumman Aerospace Corporation, CN-59, Forrestal Campus, Princeton, NJ 08544
176. P. M. Stone, Office of Fusion Energy, Office of Energy Research, ER-532 Germantown, U.S. Department of Energy, Washington, DC 20545
177. I. N. Sviatoslavsky, Room 33, Engineering Research Building, 1500 Johnson Drive, University of Wisconsin, Madison, WI 53706
178. R. E. Tatro, Manager, Energy Systems, M.Z. 16-1070, General Dynamics-Convair Division, P.O. Box 80847, San Diego, CA 92138
179. F. Thomas, B-20-5, Grumman Aerospace Corporation, Bethpage, NY 11714
180. K. I. Thomassen, Lawrence Livermore National Laboratory, P.O. Box 5511, Livermore, CA 94550
181. R. J. Thome, Francis Bitter National Magnet Laboratory, 170 Albany Street, Cambridge, MA 02139
182. C. Trachsel, McDonnell Douglas Astronautics Company, P.O. Box 516, St. Louis, MO 63166
183. A. W. Trivelpiece, Office of Energy Research, U.S. Department of Energy, Washington, DC 20545
184. L. R. Turner, Fusion Power Program, Argonne National Laboratory, 9700 South Cass Avenue, Argonne, IL 60439
185. E. H. Valeo, Princeton Plasma Physics Laboratory, P.O. Box 451, Princeton, NJ 08544
186. R. Varma, Physical Research Laboratory, Navrangpura, Ahmedabad 380009, India
187. K. E. Wakefield, Princeton Plasma Physics Laboratory, P.O. Box 451, Princeton, NJ 08544
188. J. C. Wesley, GA Technologies, Inc., P.O. Box 81608, San Diego, CA 92138

189. J. E. C. Williams, Francis Bitter National Magnet Laboratory, 170 Albany Street, Cambridge, MA 02139
190. H. H. Yoshikawa, W/A-62, Hanford Engineering Development Laboratory, P.O. Box 1970, Richland, WA 99352
191. K. M. Young, Princeton Plasma Physics Laboratory, P.O. Box 451, Princeton, NJ 08544
192. N. E. Young, Princeton Plasma Physics Laboratory, P.O. Box 451, Princeton, NJ 08544
193. Bibliothek, Max-Planck Institut fur Plasmaphysik, D-8046 Garching, Federal Republic of Germany
194. Bibliothek, Institut fur Plasmaphysik, KFA, Postfach 1913, D-5170 Julich, Federal Republic of Germany
195. Bibliotheque, Service du Confinement des Plasmas, CEA, B.P. No. 6, 92 Fontenay-aux-Roses (Seine), France
196. Documentation S.I.G.N., Department de la Physique du Plasma et de la Fusion Controlee, Association EURATOM-CEA, Centre d'Etudes Nucleaires, B.P. 85, Centre du Tri, 38041 Grenoble, Cedex, France
197. Library, Centre de Recherches en Physique des Plasmas, 21 Avenue des Bains, 1007 Lausanne, Switzerland
198. Library, Culham Laboratory, UKAEA, Abingdon, Oxfordshire, OX14 3DB, England
199. Library, FOM Instituut voor Plasma-Fysica, Rijnhuizen, Edisonbaan 14, 3439 MN Nieuwegein, Netherlands
200. Library, Institute of Physics, Academia Sinica, Beijing, People's Republic of China
201. Library, Institute for Plasma Physics, Nagoya University, Nagoya 464, Japan
202. Library, International Centre for Theoretical Physics, Trieste, Italy
203. Library, JET Joint Undertaking, Abingdon, Oxfordshire, OX14 3DB, England
204. Library, Laboratorio Gas Ionizzati, CP 56, I-00044 Frascati, Rome, Italy
205. Plasma Research Laboratory, Australian National Laboratory, P.O. Box 4, Canberra, ACT 2000, Australia
206. Thermonuclear Library, Japan Atomic Energy Research Institute, Tokai, Naka, Ibaraki, Japan
207. Library, Plasma Physics Laboratory, Kyoto University, Gokasho, Uji, Kyoto, Japan
208. Office of the Assistant Manager for Energy Research and Development, U.S. Department of Energy, Oak Ridge Operations, P.O. Box E, Oak Ridge, TN 37831

210–385. Given distribution as shown in TIC-4500, Magnetic Fusion Energy (Distribution Category UC-20 c,d: Reactor Materials and Fusion Systems)